Available online at www.sciencedirect.com
SCIENCE DIRECT®
Journal of Luminescence 114 (2005) 137–144
JOURNAL OF LUMINESCENCE
www.elsevier.com/locate/jlumin

Quenching of Si nanocrystal photoluminescence by doping with gold or phosphorous

Anna L. Tchebotareva[a,*], Michiel J.A. de Dood[a], Julie S. Biteen[b], Harry A. Atwater[b], Albert Polman[a,b]

[a]*FOM Institute for Atomic and Molecular Physics, Kruislaan 407, 1098 SJ Amsterdam, The Netherlands*
[b]*California Institute of Technology, 1200 E. California Blvd., Pasadena, CA 91125, USA*

Received 15 April 2004; received in revised form 10 November 2004; accepted 20 December 2004
Available online 19 February 2005

Abstract

Si nanocrystals embedded in SiO_2 doped with P and Au at concentrations in the range of 1×10^{18}–$3 \times 10^{20}\,cm^{-3}$ exhibit photoluminescence quenching. Upon increasing the Au concentration, a gradual decrease in nanocrystal photoluminescence intensity is observed. Using a statistical model for luminescence quenching, we derive a typical radius of ~3 nm for nanocrystals luminescing around 800 nm. Au doping also leads to a luminescence lifetime reduction, which is attributed to energy transfer between adjacent Si nanocrystals, possibly mediated by the presence of Au in the form of ions or nanocrystals. Doping with P at concentrations up to $3 \times 10^{19}\,cm^{-3}$ leads to a luminescence enhancement, most likely due to passivation of the nanocrystal–SiO_2 interfaces. Upon further P doping the nanocrystal luminescence gradually decreases, with little change in luminescence lifetime.

PACS: 78.67.Bf; 78.67.Hc; 68.55.Ln

Keywords: Photoluminescence; Quenching

1. Introduction

During the last decade, a large amount of research was devoted to the creation of alternative methods of obtaining an efficient light source based on silicon. It was found that Si quantum dots emit light at visible and near-infrared wavelengths. This luminescence was first observed in porous silicon [1,2], a material that consists of a sponge-like network of partially oxidised small Si crystallites. After this discovery, many alternative methods, including ion implantation of Si into SiO_2 [3–6] and sputter deposition of Si-rich

*Corresponding author. Tel.: +31 20 608 1234; fax: +31 20 608 4106.
E-mail address: a.tchebotareva@amolf.nl (A.L. Tchebotareva).

0022-2313/$ - see front matter © 2005 Elsevier B.V. All rights reserved.
doi:10.1016/j.jlumin.2004.12.014

SiO_2 [7–10], were developed to create Si nanocrystals embedded in SiO_2. These systems allow the effects of the complex nanostructure and of ambient effects on surface passivation to be eliminated. Independent experiments on samples prepared by different methods demonstrated that the broad-band emission from Si quantum dots at red to near-IR wavelengths ($\lambda > 650$ nm) are due to a quantum confinement effect [4,5,11,12]. For ensemble measurements on these indirect band gap semiconductor quantum dots, the large spectral width (>100 nm) typically observed for emission is due to both inhomogeneous broadening and homogeneous broadening [13]. Despite a large amount of work on the optical characterization of Si nanocrystals, the exact relation between size and emission energy remains unknown. This is first of all due to the fact that optical measurements are most often performed on ensembles of nanocrystals with a broad size distribution. The size distribution of such samples can be analyzed by transmission electron microscopy (TEM). However, due to the low contrast of electron densities in Si and SiO_2, TEM analysis can give only a rough estimate of the diameter of the studied Si nanocrystals. This makes size measurements of nanocrystals inaccurate. Furthermore, the total size distribution of nanocrystals estimated by TEM does not provide any information about the size distribution of *optically active* nanocrystals. This quantity depends critically on sample preparation conditions such as annealing and passivation treatment.

One way to address the relation between size and emission energy is to begin with a fixed reference sample and then change the size distribution of optically active nanocrystals in a controlled way. By comparing photoluminescence (PL) spectra for different distributions of optically active nanocrystals, one can acquire information regarding the relation between size and emission energy of optically active nanocrystals. To do so, we dope an ensemble of optically active nanocrystals with luminescence quenching ions, each of which could quench the luminescence of a single nanocrystal. For this purpose, we choose gold, which is known to produce an efficient deep recombination trap state in crystalline silicon [14]. Assuming that Au atoms produce a similar deep trap in nanocrystals, one would expect the luminescence from Si nanocrystals to be quenched by Au doping. Another scheme to quench Si nanocrystal luminescence, but in a different way, uses the introduction of dopants such as phosphorous. In bulk Si, the donor ionization energy level of P is situated close to the conduction band. Hence at room temperature, P provides a free electron in Si, leading to its well-known doping effect. In an analogous way, P atoms located inside a Si nanocrystal can provide an extra electron. This carrier would quench the PL by the annihilation of an optically generated exciton through Auger recombination [15,16].

The aim of this study is to investigate the quenching effect of both Au and P atoms on the PL of Si nanocrystals. We introduce a uniform distribution of each quencher throughout SiO_2 films containing Si nanocrystals produced by ion implantation. We use a statistical model to describe the probability that a nanocrystal will contain a quencher, assuming that it depends only on the quencher concentration and the nanocrystal size. We find that the PL can indeed be quenched in a controlled way, with strikingly different effects for Au-doped and P-doped samples. The experimental data cannot be fully described by the statistical model, indicating that homogeneous broadening and interactions between Si nanocrystals may need to be taken into account.

2. Model

The optical emission of Si nanocrystals under optical pumping occurs via a series of processes. First, an electron is excited from the valence band to one of the higher-lying electronic levels in the conduction band of the nanocrystal, leaving a hole behind. Subsequently, on a time scale faster than a picosecond, the electron and hole relax to their minimum energy states to form an exciton bound inside the Si nanocrystal. The exciton recombines on a time scale varying from tens of microseconds at 300 K to several milliseconds at 10 K [17]. This recombination is accompanied by the emission of a photon with an energy characteristic of the

excitonic state. At present, the nature of the excitonic state is unknown. It may be centered in the nanocrystals (the "classical" model for exciton recombination in semiconductor quantum dots), or alternatively, it could be bound at a localized surface state [18]. In both cases the exciton wave function not only entirely overlaps with the Si nanocrystal, but also penetrates into the surrounding SiO_2 matrix (the exciton Bohr radius in bulk Si is ~5 nm).

Controlled size-dependent quenching may be achieved by doping the nanocrystals with atoms or ions, using dopants such as Au or P, assuming that these dopants lead to recombination paths with rates faster than the excitonic decay rate. Since a P atom inside SiO_2 acts as a network modifier and does not provide free electrons, the dopant has to be incorporated in the nanocrystal itself in order to be effective. When a uniform concentration of dopants is introduced into a sample containing nanocrystals, the probability of doping a nanocrystal depends on the dopant concentration and the size of the nanocrystal. The probability that a nanocrystal with a volume V_{nc} will contain k dopants in the presence of a uniform concentration of dopants n, is given by the Poissonian distribution:

$$P(k) = \frac{e^{-V_{nc}n}(V_{nc}n)^k}{k!}. \quad (1)$$

Assuming that a single dopant inside a nanocrystal completely quenches all the PL emission of that nanocrystal, all nanocrystals containing at least one dopant will not emit light. Hence, the probability that a nanocrystal will be optically active in a sample with dopants is given by the probability of having no dopants inside this nanocrystal:

$$P(k = 0) = e^{-V_{nc}n}. \quad (2)$$

This probability calculated for spherically shaped nanocrystals is plotted in Fig. 1 as a function of nanocrystal radius for different dopant concentrations ranging from 3×10^{17} to 3×10^{19} at/cm^3. This graph demonstrates that at a given dopant concentration, larger nanocrystals (long-wavelength side of emission spectrum) are doped and hence should be optically inactive, while most of the smaller ones (short-wavelength side of emission spectrum) remain undoped so that this majority can still emit light. Hence, it is expected that doping of Si nanocrystals with quenchers will cause a decrease in intensity combined with an overall blue shift of the PL emission spectrum. By varying the concentration of quenchers, it would then be possible to tailor the size distribution of optically active nanocrystals and to relate the PL emission wavelength directly to nanocrystal size. Note that the analysis described in this section is independent of the number density of Si nanocrystals in the SiO_2 matrix.

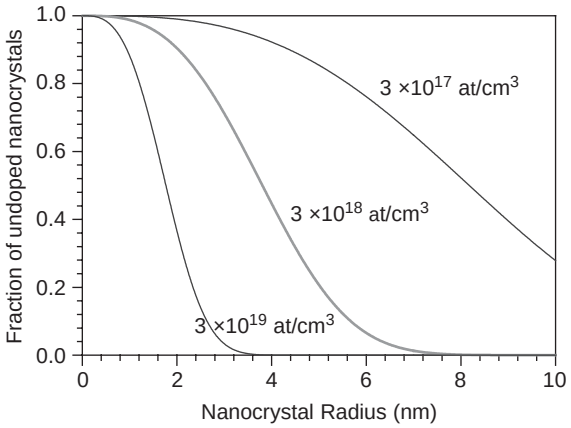

Fig. 1. Calculated probability that a spherical nanocrystal will contain no dopants (i.e., that it will remain optically active) as a function of the nanocrystal's radius. Data are shown for quencher concentrations of 3×10^{17}, 3×10^{18} and 3×10^{19} at/cm^3.

3. Experimental

50-keV Si ions were implanted into a 100-nm-thick thermally grown SiO_2 layer on Si(1 0 0) to a total fluence of 5×10^{16} Si/cm^2, thus forming a supersaturated solution of Si in SiO_2. After this, Si nanocrystals were formed by thermal annealing of the samples at 1100 °C for 10 min in an Ar flow [4,12]. After annealing, either Au or P dopants were introduced uniformly into the SiO_2 layer by a series of ion implantations. The energies and fluences for each implantation were chosen so as to yield to a uniform concentration profile. Ions of

both kinds were implanted at five different energies, which ranged from 12 to 277 keV for Au, and from 5 to 65 keV for P. Samples containing six different Au or P concentrations between 1×10^{18} and 3×10^{20} atoms/cm^3 (0.0015–0.45 at%) were prepared. Subsequent annealing for 10 min at 800 °C in a (92% N_2 + 8% H_2) flow was performed in order to passivate the Si nanocrystals and to suppress luminescence from defects produced during the ion implantation process [3].

The optical properties of samples were studied by PL. The samples were excited using the $\lambda = 488$ nm line of an Ar-ion laser, modulated on–off at a frequency of 149 Hz using an acousto-optical modulator. The luminescence from the samples was collected by a 15 cm focal length lens and focused on the entrance slits of a 48 cm monochromator. A photomultiplier tube in combination with a lock-in amplifier was used to record the PL spectra, while a photon counting technique was used to record lifetime traces of the nanocrystals at a fixed wavelength. The time resolution of the setup was <300 ns, limited by the acousto-optical modulator.

4. Results and discussion

4.1. Doping of Si nanocrystals with Au

Room-temperature PL spectra of samples with different concentrations of Au atoms are shown in Fig. 2 along with the spectrum of a sample without dopants. A significant decrease of the PL intensity at all wavelengths is observed as the Au concentration increases above 1×10^{18} atoms/cm^3, with an almost complete quenching of the nanocrystal emission at the highest Au concentration (3×10^{19} cm^{-3}). Fig. 3 shows PL decay curves measured at the peak PL emission wavelength ($\lambda = 800$ nm) for the undoped and Au-doped samples. These data are well described by a stretched exponential function, $I = I_0 \exp[-(t/\tau)^{\beta}]$, with I_0 being the steady-state PL intensity at the moment of switching the pump laser off. The PL of the undoped sample shows a decay time of $\tau = 53$ μs and $\beta \approx 0.7$. These values are similar to those found in previous studies of Si nanocrystals made by ion implantation [4,12]. For increasing Au concentration inside the SiO_2 layer, the lifetime τ gradually decreases from ~53 μs for the undoped sample to ~7 μs for the sample containing 3×10^{19} Au/cm^3. Besides inducing changes in lifetime, the presence of Au also induces

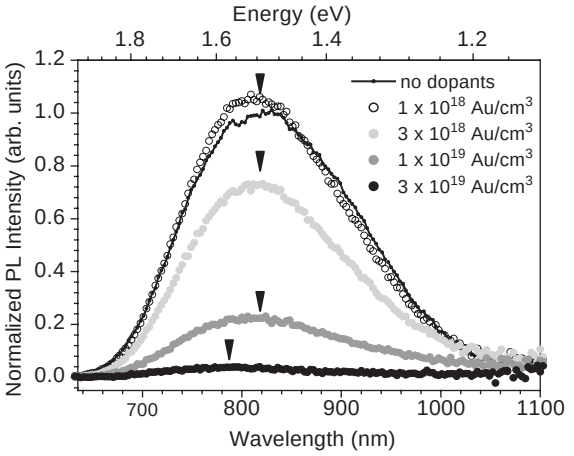

Fig. 2. Room temperature PL spectra of Si nanocrystal doped SiO_2 films doped with different concentrations of Au atoms. Pump wavelength $\lambda = 488$ nm. The arrows indicate the positions of the maxima of the measured spectra.

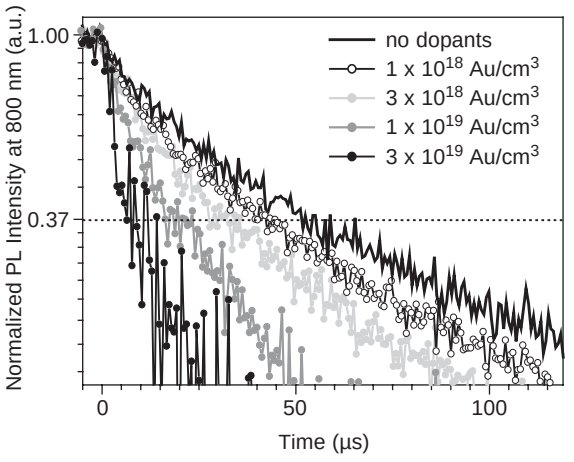

Fig. 3. Room temperature PL decay traces of Si nanocrystal doped SiO_2 films doped with different concentrations of Au atoms. The 488-nm pump was switched off at $t = 0$. A reference trace (no Au doping) is also shown. The dotted line indicates the 1/e value.

a slight blue shift of the emitted PL for the highest Au concentration (peak PL wavelengths are indicated with arrows in Fig. 2). This blue shift is consistent with the preferential doping of large Si nanocrystals described in Section 2, resulting in quenching of their PL emission, i.e., of the long-wavelength part of the PL spectrum, but is much smaller than expected based on the simple model as will be discussed below.

The change in lifetime demonstrated by Fig. 3 is not anticipated by the statistical model introduced in Section 2. This model assumes that a doped nanocrystal is fully optically inactive and thus does not contribute to the detected PL signal. One possible explanation for the observed decrease in lifetime may be the effect of coupling (energy transfer) between the densely packed nanocrystals. In this case, a quenched nanocrystal would also affect the lifetime of neighboring nanocrystals, leading to a reduction (but not full quenching) of the latter. Coupling between Si nanocrystals has been previously observed in experiments where the nanocrystal density was varied, and the stretched exponential decay behavior is thought to be a signature of such interaction [12].

The lifetime reduction with increasing Au concentration in Fig. 3 is due to an increase in non-radiative decay rate and is at least partially responsible for the decrease in the PL intensity in Fig. 2. The PL from the nanocrystals is directly proportional to the number of nanocrystals in the excited state times the radiative rate ($1/\tau_{.d}$) of the excited state. The radiative lifetime $\tau_{.d}$ is an intrinsic property of the nanocrystal and is expected to be independent of the concentration of dopants. The excited state population n_1 can be deduced from a rate equation model that treats each nanocrystal as an effective two-level system. Under steady-state conditions (continuous wave pumping) this leads to

$$\frac{dn_1}{dt} = W(n - n_1) - \frac{n_1}{\tau} = 0,$$

where n is the total number of nanocrystals, τ is the total lifetime of the excited state, and W is the pump rate from the ground to excited state. In the low pump power limit ($W << 1/\tau$), the excited state population is given by $n_1 = Wn\tau$. The PL intensity is thus proportional to $Wn\tau/\tau_{.d}$. Consequently, the product of PL intensity and measured decay rate ($1/\tau$) is a measure of the number of optically active nanocrystals n.

Fig. 4 shows this product of the PL intensity and decay rate ($1/\tau$) at 800 nm as a function of the Au concentration. As can be seen, except for a small initial increase for the lowest Au concentration, the total density of optically active nanocrystals decreases with increasing Au concentration. This proves that Au is an effective quencher of excited nanocrystals.

It was previously demonstrated that defects/damage resulting from ion implantation can render nanocrystals optically inactive [19]. In order to verify that the observed quenching effect is induced by the implanted Au ions and is not due to residual damage from the ion implantation process, a number of samples containing Si nanocrystals were implanted with 2 MeV Xe ions at various fluences. The projected range of the Xe ions was larger than the thickness of the SiO_2 layer, and the implantation fluences were chosen in such a way that the resulting damage (i.e., the average number of atomic displacements per Xe ion) in the SiO_2 layer was comparable to or higher than the damage produced by the Au implantations. PL measurements on Xe-implanted samples (not

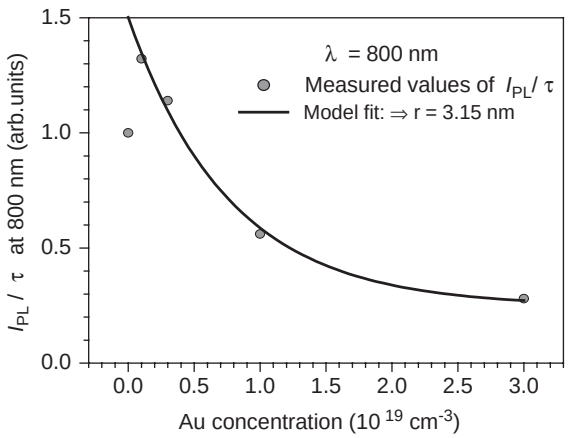

Fig. 4. PL intensity divided by 1/e decay time of Si nanocrystal doped SiO_2 films doped with different concentrations of Au atoms. These data are derived from data in Figs. 2 and 3 and provide a measure of the number of active Si nanocrystals as a function of Au doping.

shown) demonstrated that, for a Xe implantation of 3×10^{15} at/cm^2 causing similar damage as in the sample with 3×10^{19} Au/cm^3, the intensity decreased by less than 50%, while the lifetime remained constant. As the sample doped with 3×10^{19} Au/cm^3 showed almost no luminescence, the observed reduction in the number of optically active nanocrystals in Au-doped samples is a true effect of the presence of Au. The decreasing trend in Fig. 4 can now be compared with the statistical model of Fig. 1. By fitting these data to Eq. (2) (which describes the probability that a nanocrystal will be optically active), one can estimate the effective radius of nanocrystals emitting light at $\lambda = 800$ nm to be $r \approx 3$ nm. This number is somewhat larger than the typical radius of 1.0–2.5 nm measured using high-resolution TEM on Si nanocrystals prepared in a similar way as described here [20]. This again is consistent with the notion that interaction between nanocrystals takes place, as this would cause the effective radius of quenched nanocrystals to be larger than their physical radius. The blue shift observed in Fig. 2 upon increased Au doping is much smaller than what would be expected according to the simple model in Section 2. This may be the result of both interaction between nanocrystals and homogeneous broadening [13].

The statistical model explains qualitatively the observed decrease of I_{PL}/τ and the blue shift of the PL spectrum in presence of high concentrations of Au dopants, but it does not provide a complete description of mechanisms responsible for the change of emission properties induced by doping with Au. Therefore, the present data are not sufficient to directly relate the emission wavelength to the size of a nanocrystal. To achieve this, further experiments should be carried out on samples with lower nanocrystal density to exclude interaction between nanocrystals.

4.2. Doping of Si nanocrystals with P atoms

Fig. 5 shows the measured PL spectra for P-doped samples. PL decay measurements taken at the peak of the PL spectrum ($\lambda = 800$ nm) are plotted in Fig. 6. The effect of P doping on nanocrystal PL differs significantly from that of

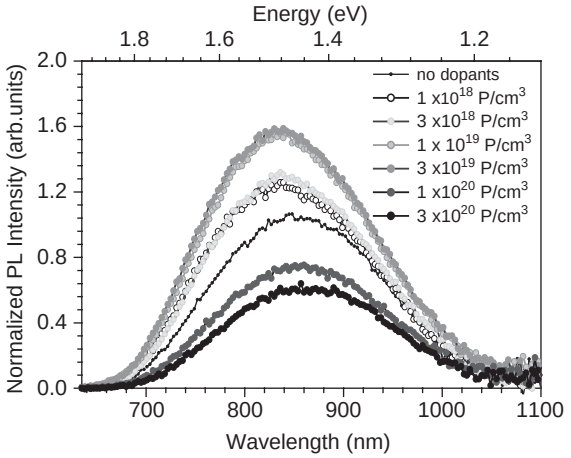

Fig. 5. Room temperature PL spectra of Si nanocrystal doped SiO_2 films doped with different concentrations of P atoms. Pump wavelength $\lambda = 488$ nm.

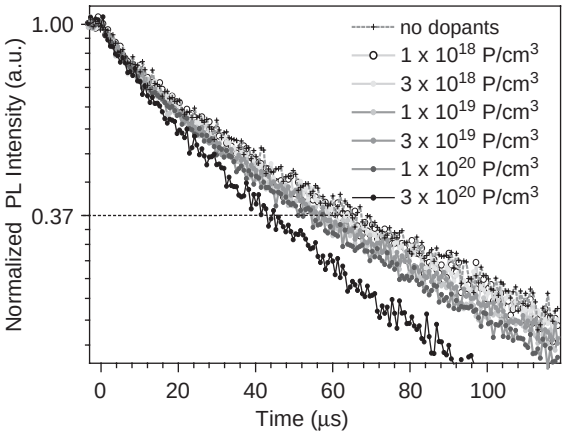

Fig. 6. Room temperature PL decay traces of Si nanocrystal doped SiO_2 films doped with different concentrations of P atoms. The 488-nm pump was switched off at $t = 0$. A reference trace (no P doping) is also shown. The dotted line indicates the 1/e value.

Au doping. Indeed, the PL measurements show that the luminescence intensity exhibits an overall increase for low P concentrations (up to 1×10^{19} cm^{-3}) (Fig. 5). When the concentration of P is increased further, the PL intensity decreases significantly, to a value of 56% relative to the intensity of the undoped sample. At the same time, the lifetime remains almost unchanged for all P concentrations (Fig. 6). This allows for a direct

interpretation of the PL intensity data without correcting for a change in lifetime. A slight decrease in lifetime is observed only for the sample with the highest P concentration ($3 \times 10^{20}\,cm^{-3}$).

The increase in PL intensity at low P concentrations may be related to the passivation of previously non-passivated Si nanocrystals. Such an effect of P has been observed earlier by Fujii et al. [21]. The initial anneal in hydrogen-containing atmosphere (92% N_2 + 8% H_2) may lead to only a partial passivation of all nanocrystals, leaving a certain fraction of them optically inactive. In such a case, passivation of Si nanocrystals by P atoms would lead to an increase in the number density of luminescent nanocrystals.

Figs. 2–5 demonstrate that the PL intensity of a sample doped with phosphorous is considerably higher than that of a sample containing the same concentration of Au atoms. This indicates that though for samples doped with P to sufficiently high concentrations the luminescence is quenched, the mechanism of this quenching differs from the one occurring in Au-doped samples. For a dopant concentration of $3 \times 10^{19}\,cm^{-3}$, the average number of dopants inside a nanocrystal of radius 3 nm, calculated using the Poisson distribution of Eq. (1), is four. At this dopant concentration, no PL was detected from the Au-doped sample, while the PL intensity of P-doped sample was still appreciable (see Fig. 5). The decrease in PL intensity, and hence the decrease in number of luminescent nanocrystals for the higher P concentrations, may be attributed to Auger recombination due to presence of P inside Si nanocrystals [16]. The Auger recombination process is much less efficient for a bound electron than for a free electron because the wavefunction of the latter inside a nanocrystal overlaps more with the wavefunction of the exciton. Hence, the efficiency of Auger recombination would be highest if all P atoms inside nanocrystals were ionized. The lower quench rate of P compared to Au could then be a result of the fact that the P dopants are only partially ionized at room temperature. Indeed, since realistic values for the ionization energy lie in the 10–100 meV range, this is the case.

Finally, we observed an initial blue shift of the PL, followed by a red shift in the samples doped with increasing P concentration. The initial blue shift may be attributed to a more effective passivation of nanocrystals close to the Si/SiO_2 interface by P atoms. These nanocrystals are initially less well passivated as the passivation is limited by diffusion of hydrogen from the surface during the forming gas anneal. It is known that these nanocrystals are smaller than average [20]. Hence, passivation of these small Si nanocrystals leads to an overall blue shift of the PL. The red shift observed at high P concentrations may be caused by the effect of P as a network modifier in SiO_2. For high P concentrations, the forming gas anneal may also lead to an increase of the average nanocrystal size causing a redshift of the PL spectrum. The presence of carriers causes the decrease in PL intensity and a blue shift. The overall shift depends on the relative contribution of the three processes (i.e. passivation, Auger recombination, and network modification of SiO_2) and is difficult to predict. This situation is distinctly different from Au-doped samples, as Au does not passivate nanocrystals, nor does it act as a network modifier in SiO_2.

Consequently, the statistical quenching model presented in Section 2 is too simple to fully describe the data. Contrary to the case of Au-doped samples, no significant lifetime change upon the increase of P concentration was observed. Assuming that the decrease in lifetime and stretched exponential behavior due to Au doping is related to interaction and energy transfer between nanocrystals, this would suggest that the presence of Au enhances energy transfer. This is not an unreasonable assumption, as Au related defects states in the silica glass or Au nanoparticles that may form by the annealing process may mediate the energy transfer. More work is required to further test this hypothesis, but if proven true, Au doping would provide an interesting way to modify and manipulate nanoscale energy transfer between Si quantum dots.

5. Conclusions

The controlled doping of Si nanocrystals embedded in SiO_2 with Au or P ions leads to

quenching of the PL intensity in two distinct ways. Gold quenches the Si nanocrystal PL at a characteristic concentration of $2 \times 10^{19}\,\mathrm{cm}^{-3}$. Comparing the measured data with a statistical model which assumes that nanocrystal PL is fully quenched by recombination at a single Au-related trap, we estimate the effective radius of Si nanocrystals emitting at 800 nm to be ~3 nm. This value is somewhat larger than that found in electron microscopy, which is attributed to interaction (energy transfer) between nanocrystals, leading to an enhanced "quench radius".

Doping Si nanocrystals with P first leads to an increased PL intensity (attributed to surface passivation), followed by a progressive decrease in PL intensity upon increased P doping. Compared to Au, a much higher fluence of P is needed to quench the PL. The quenching effect of P may be related to Auger quenching due to carriers from partially ionized P donors inside nanocrystals. We also find that doping with Au leads to a reduction in PL lifetime, while doping with P does not. This may indicate that Au, either in the form of ions or nanocrystals, may mediate and enhance energy transfer between Si nanocrystals.

Acknowledgements

The authors are thankful to Dr. M. Fujii for stimulating discussions. This work is part of the research program of the Foundation for Fundamental Research on Matter (FOM) which is financially supported by Dutch organization for Scientific Research (NWO). A.T. acknowledges the financial support from Fonds NATEQ (Québec, Canada) over the course of this research. Research at Caltech was supported by the National Science Foundation.

References

[1] L.T. Canham, Appl. Phys. Lett. 57 (1990) 1049; V. Lehmann, U. Gösele, Appl. Phys. Lett. 58 (1991) 856.
[2] A.G. Cullis, L.T. Canham, P.D.J. Calcott, J. Appl. Phys. 82 (1997) 909 and references therein.
[3] T. Shimizu-Iwayama, M. Ohshima, T. Niimi, S. Nakao, K. Saitoh, T. Fujita, N. Itoh, J. Phys. Condens. Matter 5 (1993) L375.
[4] K.S. Min, K.V. Shcheglov, C.M. Yang, H.A. Atwater, M.L. Brongersma, A. Polman, Appl. Phys. Lett. 69 (1996) 2033.
[5] T. Komoda, J. Kelly, F. Cristiano, A. Nejim, P.L.F. Hemment, K.P. Homewood, R. Gwilliam, J.E. Mynard, B.J. Sealy, Nucl. Instr. Meth. B 96 (1995) 387.
[6] H.M. Cheong, W. Paul, S.P. Withrow, J.G. Zhu, J.D. Budai, C.W. White, D.M. Hembree Jr., Appl. Phys. Lett. 66 (1995) 851.
[7] Q. Zhang, S.C. Bayliss, D.A. Hutt, Appl. Phys. Lett. 66 (1995) 1977.
[8] S. Nozaki, H. Nakamura, H. Oho, H. Morisaki, N. Itoh, Japan J. Appl. Phys.-II 34 (Suppl. 34-1) (1994) 122.
[9] S. Chavret, R. Madelon, R. Rizk, B. Garrido, O. Gonzalez-Varona, M. Lopez, A. Perez-Rodriguez, J.R. Morante, J. Lumin. 80 (1998) 241.
[10] L. Tsybeskov, K.D. Hirschmann, S.P. Duttagupta, P.M. Fauchet, M. Zacharias, J.P. McCaffey, D.J. Lockwood, Phys. Stat. Solidi A 165 (1998) 69.
[11] P.D.J. Calcott, K.J. Nash, L.T. Canham, M.J. Kane, D. Bramhead, J. Phys.: Condens. Matter 5 (1993) L91.
[12] F. Priolo, G. Franzò, D. Pacifici, V. Vinciguerra, F. Iacona, A. Irrera, J. Appl. Phys. 89 (2001) 264.
[13] J. Valenta, R. Juhasz, J. Linnros, Appl. Phys. Lett. 80 (2002) 1070.
[14] S.M. Sze, Physics of Semiconductor Devices, Wiley, New York, 1981.
[15] M. Lannoo, C. Delerue, G. Allan, J. Lumin. 70 (1996) 170.
[16] A. Mimura, M. Fujii, S. Hayashi, D. Kovalev, F. Koch, Phys. Rev. B 62 (2000) 12625.
[17] M.L. Brongersma, P.G. Kik, A. Polman, K.S. Min, H. Atwater, Appl. Phys. Lett. 76 (2000) 351.
[18] M.V. Wolkin, J. Jorne, P.M. Fauchet, G. Allan, C. Delerue, Phys. Rev. Lett. 82 (1999) 197.
[19] D. Pacifici, E.C. Moreira, G. Franzò, V. Martorino, F. Priolo, Phys. Rev. B 65 (2002) 144109-1.
[20] M.L. Brongersma, A. Polman, K.S. Min, H.A. Atwater, J. Appl. Phys. 86 (1999) 759.
[21] M. Fujii, A. Mimura, S. Hayashi, K. Yamamoto, Appl. Phys. Lett. 75 (1999) 184.